Microstructure evolution in a Cu-Cr-Zr alloy during warm intense plastic straining

2014 IOP Conf. Ser.: Mater. Sci. Eng. 63 012094

(http://iopscience.iop.org/1757-899X/63/1/012094)

IOP Conf. Series: Materials Science and Engineering **63** (2014) 012094 doi:10.1088/1757-899X/63/1/012094

Microstructure evolution in a Cu-Cr-Zr alloy during warm intense plastic straining

R Mishnev[1], I Shakhova, A Belyakov and R Kaibyshev
[1] Belgorod State University, Pobeda 85, Belgorod 308015, Russia
E-mail: mishnev@bsu.edu.ru

Abstract. The effect of equal channel angular pressing at a temperature of 200 °C to a total strain of 12 on microstructure evolution and mechanical properties of a Cu-0.87wt.%Cr-0.06wt.%Zr was investigated. New ultrafine grains resulted from gradual increase in the misorientations of strain-induced low-angle boundaries with increasing number of passes. Therefore, the development of ultrafine grains is considered as a kind of dynamic recrystallization. The equal channel angular pressing to a total strain of 12 resulted in the formation of almost equiaxed ultrafine grained structure with an average grain size of 0.5 □m and 0.7 □m in the solution treated and aged samples, respectively. At the same time, the fraction of ultrafine grains comprises 0.77 in the solution treated samples and 0.72 in the aged samples. Significant grain refinement led to the remarkable increase of the ultimate tensile strength up to 550 MPa.

1. Introduction

The mechanical properties of metallic materials, in particularly, strength, are strongly affected by their microstructures. In consequence, the grain refinement can significantly enhance the strength. The most effective method to obtain the ultrafine grained metals and alloys is intense plastic straining [1-3]. The mechanisms of structural changes during thermo-mechanical processing are of great practical and theoretical interests. The major mechanism responsible for the microstructure evolution during large plastic deformation is dynamic recrystallization [4]. Studying the regularities of dynamic recrystallization should allow us to control the formation of microstructure during plastic working and correspondingly, the mechanical properties of metallic materials. Nowadays, two types of dynamic recrystallization are discussed in the literature [4-6]. The microstructure evolution during hot deformation at temperature above $0.5T_m$ is usually resulted from discontinuous dynamic recrystallization (dDRX) [5]. On the other hand, the formation of new ultrafine grains at low-to-moderate temperature (below $0.5T_m$) is considered as a type of continuous dynamic recrystallization (cDRX) [6]. The main characteristics of dDRX have been sufficiently clarified. In contrast, the investigation of microstructure evolution during cold-to-warm plastic deformation is complicated and, therefore, the structural changes leading to the formation of ultrafine grains have not been studied in detail. The formation of new ultrafine grains occurs due to progressive increase in the misorientations of strain-induced subboundaries from low-angle misorientation to typical values of conventional high-angle boundaries upon plastic working [6, 7]. The present research work was aimed to study the microstructure evolution and the mechanical properties in a Cu-Cr-Zr alloy during warm equal channel angular pressing.

2. Experimental Procedure

An alloy of Cu-0.87wt.% Cr-0.06 wt.% Zr was used. Two types of samples were prepared. The first set of samples was subjected to the solution treatment (ST) at a temperature of 920 °C for 30 min followed by water quenching. The second set of samples was subjected additionally to aging at a temperature of 450 °C for 4 h and these samples are denoted as ST+AT. The billets with starting dimension 14 mm × 14 mm × 80 mm were subjected to ECAP at temperature of 200 °C via so-called route B_C (90° anticlockwise rotation of the specimens after each pass) to total strains of 1, 2, 4, 8 and 12. A die angle of 90° was

chosen, resulting in a true strain of about 1 at each pass. The microstructural investigations were performed on the Y plane, i.e. flow plane parallel to the side face at the point of exit from the die [8], using a Quanta 250 Nowa scanning electron microscope (SEM) equipped with an electron backscattering diffraction (EBSD) analyzer incorporating an orientation imaging microscopy (OIM). The SEM samples were electropolished using an electrolyte of HNO3:CH3OH=1:3 at temperature of -10 °C with a voltage of 10 V. The EBSD scanning was performed with a step size of 100 nm for the samples processed by 1 and 2 ECAP passes and 60 nm for the samples subjected to 4, 8 and 12 ECAP passes. The mean grain size was measured by linear intercept method on the OIM images counting the distance between high-angle boundaries. The critical value of misorientation for the high-angle boundaries was chosen 15°. The fraction of ultrafine grains (UFG) with a size below 2 □m was obtained using IOM software (EDAX TSL, version 5.2). The mechanical properties were determined by means of tensile testing. The mechanical tests were performed using an Instron 5882 testing machine at room temperature.

3. Results and Discussion

3.1 Microstructure evolution.

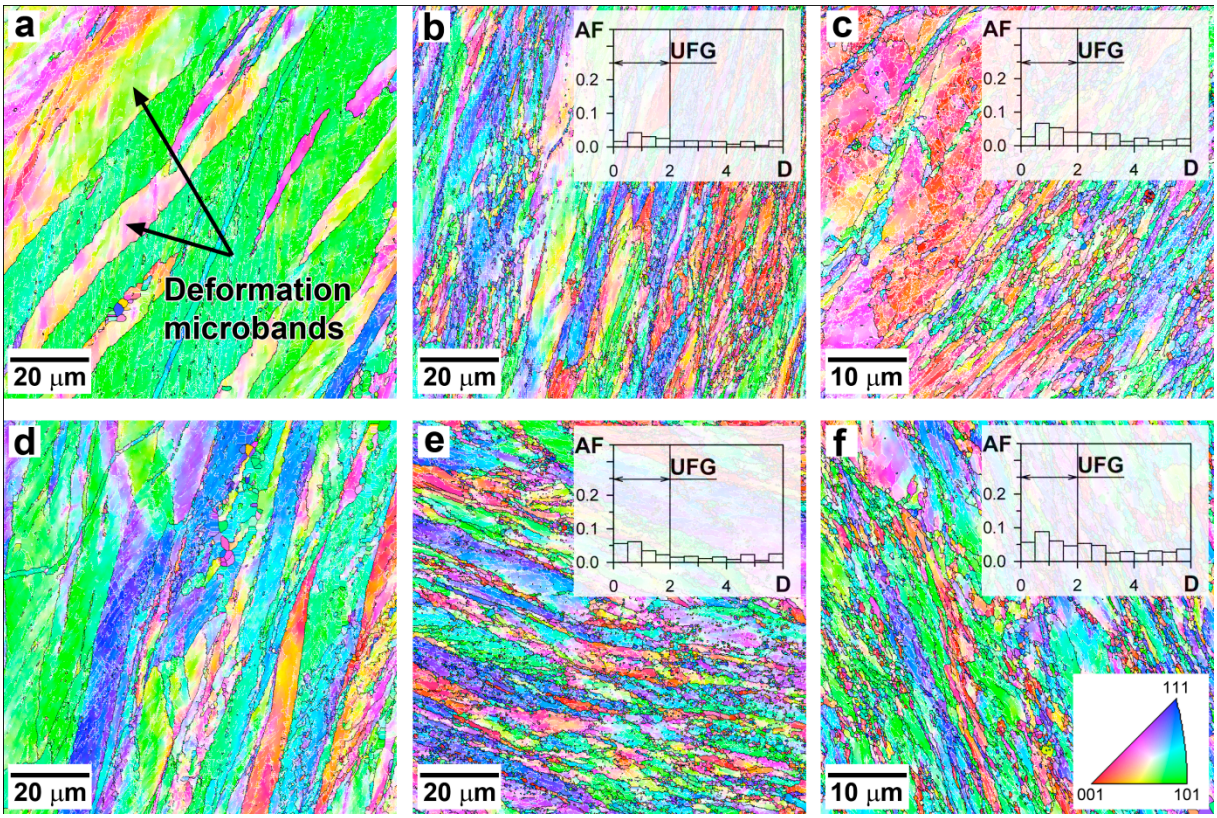

Figure 1. Deformation microstructures and grain size distributions evolved in the solution treated (ST) (a, b, c) and aging treated (ST+AT) (d, e, f) samples during an equal channel angular pressing at temperature of 200 °C to total strains of 1 (a, d); 2 (b, e) and 4 (c, f). The white and black lines indicate the low- and high-angle boundaries, respectively. The inverse pole figures are shown for the transverse direction. The AF, D and UFG on the grain size distributions indicate the Area Fraction, the Grain Size (μm) and the Ultrafine Grains, respectively.

The deformation microstructures developed in a Cu-Cr-Zr alloy under ECAP to total strains of 1, 2 and 4 are shown in figure 1. Generally, the first ECAP pass is accompanied by the elongation of the original grains and also brings about the development of a large number of low-angle strain-induced subboundaries (figures 1a and 1d). Note here that the fraction of low-angle boundaries is larger in the ST+AT state than in the ST state. The deformation microbands are formed within initial grains in the ST state in addition to the strain-induced subboundaries (figure 1a). The well-defined cell-type substructures are evolved within the original grains in both the ST and ST+AT samples after the second ECAP pass (figures 1b and 1e). These substructures are characterized by low-angle misorientations. The second ECAP pass is also accompanied by the development of almost equiaxed new ultrafine grains nearby the initial grain boubdaries. It is clearly seen from the corresponding grain size distribution (figures 1b and 1e) that the fraction of new ultrafine grains (UFGs) with a mean size below 2 μm, is larger in the ST+AT state in comparison with ST ones. Note here that the deformation microstructure of ST+AT samples consists of finer grains. The area fractions of grains with average size of 0.25 μm and 0.75 μm comprise 0.05 and 0.06, respectively (figure 1e). However, in the ST sample, the corresponding fractions of grains of the same size are much smaller and do not exceed 0.02 and 0.04 (figure 1b).

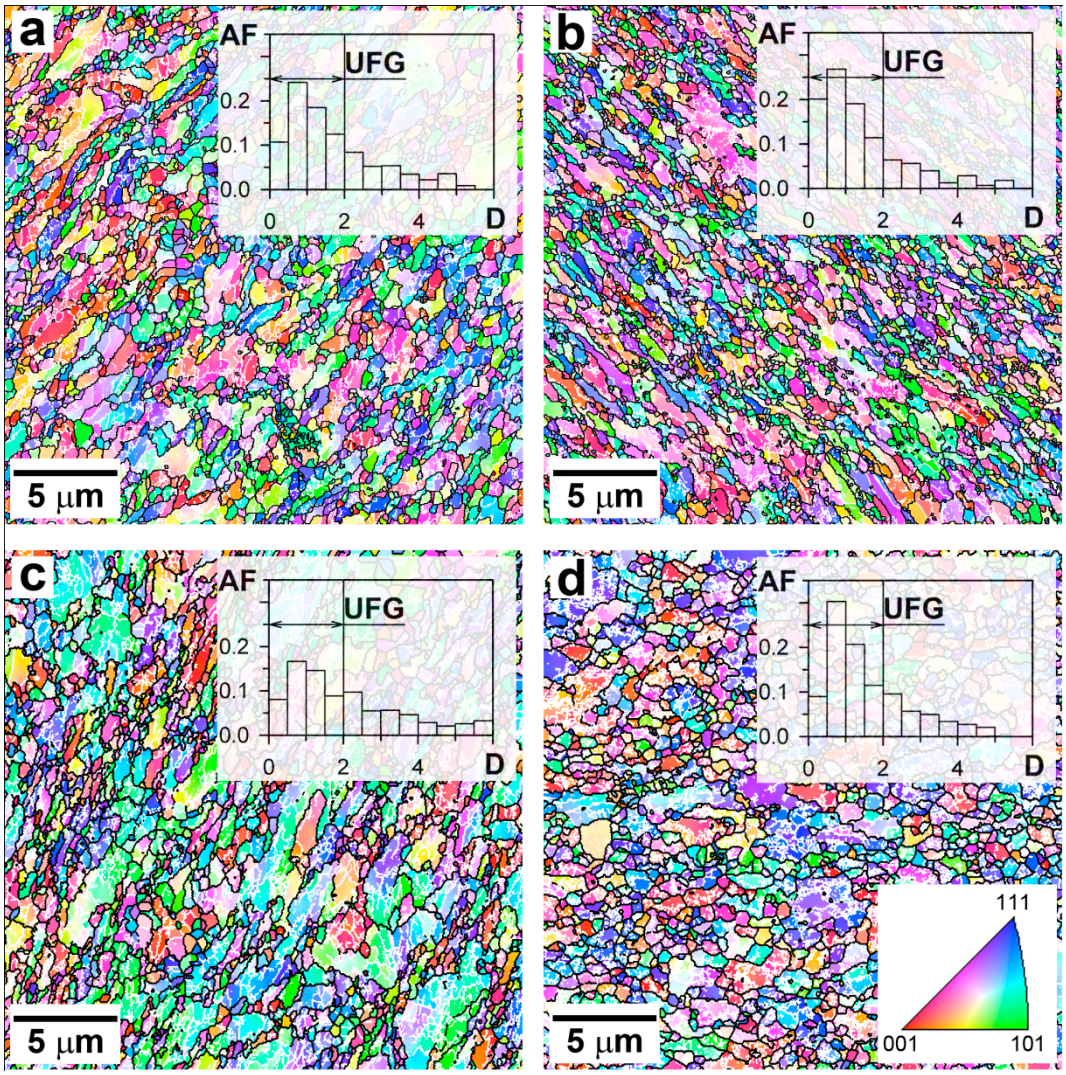

Figure 2. Deformation microstructures and grain size distributions in the solution treated (ST) (a, b) and aging treated (ST+AT) (c, d) samples subjected to equal channel angular pressing at 200 °C to strains of 8 (a, c) and 12 (b, d). The white and black lines indicate the low- and high-angle boundaries, respectively. The inverse pole figures are shown for the transverse direction. The AF, D and UFG on the grain size distributions indicate the Area Fraction, the Grain Size (μm) and the Ultrafine Grains, respectively.

Upon further straining to 4, the number of ultrafine grains increases resulting in the formation of a necklace like structure (figures 1c and 1f). The new grains are surrounded by moderate-to-high boundaries and these grains appear as chains between coarser remainders of the initial grains. The ST+AT samples demonstrate the faster rate of the formation of UFGs and these grains are finer in comparison with the ST samples. This effect of the initial state on the development of UFG becomes opposite after increase of the number of passes to 8. It is seen from figure 2 that remarkable grain refinement occurs upon further ECAP process despite of the difference in the initial states. Note here that deformation microstructures look quite similar: the reminders of the original grains are separated by the areas of the ultrafine grains (figures 2a and 2c). The main distinguishing feature of ST+AT samples is larger size of the remainders of the original grains (about 4 μm) as compared to that (3 μm) in the ST samples. As a result, the ECAP to a strain of 8 leads to the appearance of sharp peak attributed to the UFGs on the corresponding grain size distributions in the ST state (figure 2a). On the other hand, the slow grain refinement in the ST+AT samples leads to the more-or-less flat-type grain size distributions after 8 ECAP passes (figure 2c). Processing to the strains of 12 results in the development of almost equiaxed ultrafine grained structures in the ST state (figure 2b). On the other hand, the microstructure of the ST+AT samples is rather heterogeneous. In addition to the ultrafine grains the final microstructure includes irregular grains with an average size of 3 μm (figure 2d). Thereby, the ST state is characterized by faster kinetic of microstructure evolution upon processing to the large strains comparing to the ST+AT state. One interesting feature of microstructure evolution should be noted. The new grains form with the constant size over the course of sequential ECAPs and only the fraction of these grains increases with increase in the strain despite of the difference in the initial state.

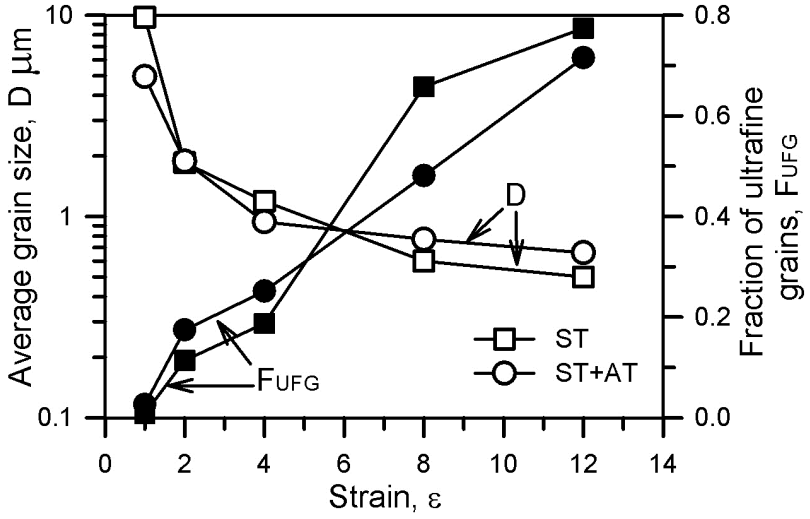

Figure 3. Effect of strain (number of ECAP passes) on the average grain size (D) and the fraction of ultrafine grains (F_{UFG}) in a Cu-Cr-Zr alloy.

Figure 3 shows the effect of ECAP at a temperature of 200 °C on the average grain size (D) and the fraction of ultrafine grains (F_{UFG}). Commonly, the change in the average grain size correlates with the fraction of ultrafine grains. The decrease in the grain size is accompanied by increase of the ultrafine grain fraction during the ECAP. After the first pass of ECAP the average grain size is 9.7 μm and 4.9 μm in the ST and the ST+AT samples, respectively. The second pass of ECAP leads to the remarkable grain refinement, the average grain size decreases to below 2 μm in both the ST and the ST+AT states. Then, the rate of grain refinement gradually decreases during further ECAP resulting in the final grain size of 0.5 μm and 0.7 μm in the ST+AT and the ST samples, respectively, after ECAP to a total strain of 12. The kinetics of new grain formation during large plastic deformation can be evaluated by the fraction of ultrafine grains (figure 3). The fraction of ultrafine grains gradually approaches 0.19 and 0.25 in the strain range $1 < \varepsilon < 4$ in the ST and the ST+AT samples, respectively. Then, the fraction of ultrafine grains demonstrates a rapid increase from 0.19 to 0.66 in the ST samples upon processing to a strain of 8 and then approach a saturation at level of about 0.8 at a large strain of 12. Such progressive increases of F_{UFG} indicates remarkable grain refinement in the ST state (see figure 2a). In contrast, the fraction of ultrafine grains almost linearly increases from 0.25 to 0.72 with increase in strain from 4 to 12 in the ST+AT samples. Therefore, the ST samples are characterized by faster kinetics of ultrafine grain formation at the large strains as compared to the ST+AT samples.

3.2 Mechanical properties

Two sets of flow curves obtained by tensile tests at room temperature for the samples processed by 1 to 12 ECAP passes are shown in figure 4. Commonly, the ECAP leads to the significant increase in strength even after the first ECAP pass as compared to the initial heat treated samples (ST and ST+AT). The strain-stress curves of ECAPed samples are characterized by a very short strain hardening range. Namely, the stresses rapidly increase to their maximum at strains of around 1% followed by gradual decrease with increasing the tensile strain up to rupture. Note here that the ST+AT samples are characterized by higher stresses than the ST samples. The tensile stresses of the ST samples gradually increase with an increase of number of ECAP passes, whereas the number of ECAP passes has not significant influence on the tensile stress for the ST+AT samples.

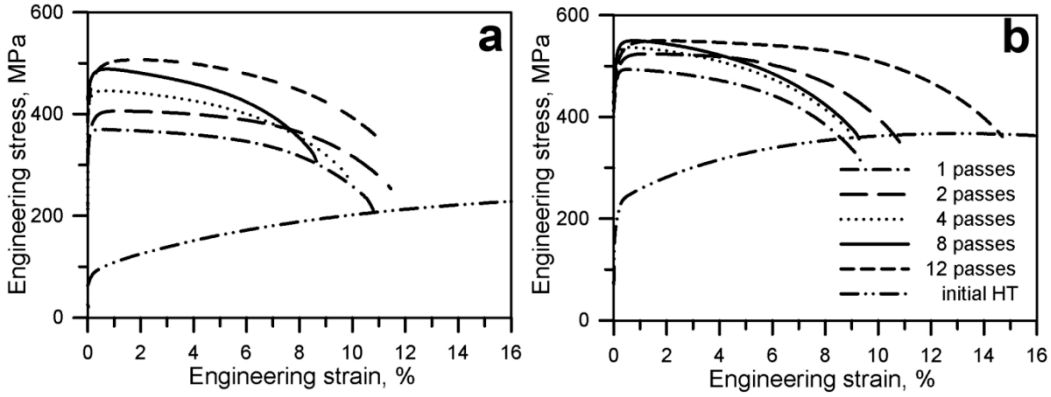

Figure 4. Engineering stress vs engineering strain curves obtained for a Cu-Cr-Zr alloy in the solution treated (ST) (a) and aging treated (ST+AT) (b) states after equal channel angular pressing at temperature of 200 °C. The initial HT corresponds to solution treatment in (a) and solution treatment + aging treatment in (b).

The effect of number of ECAP passes on the strength and elongation is shown in figure 5. Note here that the yield stress ($\sigma_{0.2}$ = 215 MPa) and ultimate tensile strength (UTS = 370 MPa) of the initial ST+AT samples are higher than those in the initial ST samples ($\sigma_{0.2}$=85 MPa and UTS=245 MPa). The initial samples are characterized by high elongation to failure of about 25% and 40% in the ST and the ST+AT states, respectively. As expected, the first ECAP pass leads to remarkable increase-in the yield stress to 370 MPa in the ST samples and 490 MPa in the ST+AT samples, while the elongation decreases to approximately 12% in the both states. Then, the yield stress/ultimate tensile strength gradually increase to 456/505 MPa and 551/550 MPa in the ST and the ST+AT samples, respectively, upon processing to the strain of 12. Note here that the elongation to rupture remains almost on the same level of 10-15% regardless of the initial states and ECAP strain. It is evident from figure 5 that the structural strengthening due to the grain refinement by ECAP superimposes on the dispersion strengthening in the ST+AT samples and, therefore, provides superior strength of the Cu-Cr-Zr alloy.

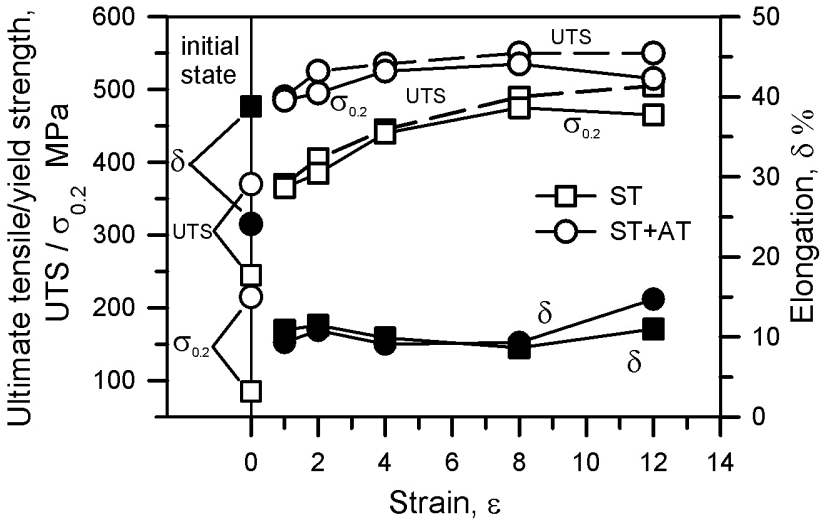

Figure 5. The effect of strain (ε) on the strength (UTS, $\sigma_{0.2}$) and elongation (δ) in a Cu-Cr-Zr alloy subjected to equal channel angular pressing at temperature of 200 °C.

4. Summary

An equal channel angular pressing of a Cu-Cr-Zr alloy to the total strain up to 12 leads to the formation of ultrafine grained structure with an average grain size of 0.5 □m and 0.7 □m in the solution treated (ST) and aging treated (ST+AT) states, respectively. The formation of new ultrafine grains occurs faster in ST+AT state after processing to the relatively small strains. Then, this behavior changes at the large strains. Namely, the ST state is characterized by the faster kinetics of the formation of ultrafine grained structure as compared to the ST+AT state. Microstructure evolution in a Cu-Cr-Zr alloy results from gradual increase in the misorientations between low-angle strain-induced subboundaries up to misorienations typical of conventional boundaries. Significant grain refinement during equal channel angular pressing accompanied by considerable increase of ultimate tensile strength to 505 MPa and 550 MPa after processing to a strain of 12 in the solution treated and aging treated states, respectively. Note here that the enhanced strength properties in the ST+AT samples are achieved by a combination of dispersion and structural strengthening.

5. Acknowledgements

The financial support received from the Ministry of Science and Education, Russia under grant No. 14.513.11.0106 is gratefully acknowledged. The authors are grateful to the personnel of the Joint Research Centre, Belgorod State University, for their assistance with instrumental analysis.

6. References

[1] Estrin Y, Vinogradov A 2013 *Acta Mater.* **61** 782
[2] Shakhova I, Dudko V, Belyakov A, Tsuzaki K, Kaibyshev R 2012 *Mater. Sci. and Eng.A* **545** 176
[3] A.P. Zhilyaev, I. Shakhova, A. Belyakov, R. Kaibyshev, T.G. Langdon 2013 *Wear* **305** 89
[4] Sakai T, Belyakov A, Kaibyshev R, Miura H, Jonas JJ 2014 *Progr. Mater. Sci.* **60** 130
[5] Sakai T, Jonas JJ 1984 *Acta Mater.* **32** 189
[6] Kobayashi C, Sakai T, Belyakov A, Miura H 2007 *Philos. Mag. Lett.* **87** 751
[7] Sakai T, Miura H, Goloborodko A, Sitdikov O 2009 *Acta Mater.* **57** 153
[8] Valiev RZ, Langdon TG 2006 *Progr. Mater. Sci.* **51** 881